J. Fluid Mech. (1979), *vol.* 94, *part* 3, *pp.* 541–559
Printed in Great Britain

Further experiments on transition to Mach reflexion

By L. F. HENDERSON AND A. LOZZI
Department of Mechanical Engineering, University of Sydney,
New South Wales 2006, Australia

(Received 3 October 1978)

Our 1975 paper reported the results of experiments on shock reflexion in a wind tunnel and a shock tube; further results are presented here. For strong shocks it is shown that transition to Mach reflexion takes place continuously at the shock wave incidence angle ω_0 corresponding to the normal shock point $\omega_0 = \omega_N$, unless the downstream boundaries form a throat. In this event transition can be promoted anywhere within the range $\omega_0 \leqslant \omega_N$, and it is even possible to suppress regular reflexion altogether! However when $\omega_0 < \omega_N$ the transition is discontinuous and accompanied by hysteresis. Again for strong shocks evidence is presented which suggests that the famous persistence of regular reflexion beyond the ω_N point $\omega_0 > \omega_N$ is spurious. For weak shocks the transition condition is not known but it is found that even for regular reflexion a marked discrepancy between theory and experiment develops as the shocks become progressively weaker. Also when weak shocks diffract over single concave corners there is a somewhat surprising discontinuity in the regular reflexion range. It seems that none of these phenomena can be adequately explained by real gas effects such as viscosity and variation of specific heats.

1. Introduction

Two principal types of wave systems may be obtained when an incident shock i reflects off a solid surface. These are regular reflexion RR and Mach reflexion MR (figures 1*a*, *b*) and they have been extensively studied, particularly in the remarkable theoretical work of von Neumann (1943). Since then other phenomena have been discovered by experiment; White (1952) noticed that the reflected shock r in MR sometimes developed a small radius bend or 'kink'. The resulting wave system is occasionally called a complex Mach reflexion CMR (figure 1*c*). At sufficiently high Mach numbers the flow downstream of r becomes supersonic and the kink may then sharpen into a slope discontinuity and be associated with an extra shock; it is sometimes called a double Mach reflexion DMR (figure 1*d*). Much experimental work has been done on these phenomena: Smith (1945); Lean (1946); White (1952); Kawamura & Saito (1956); Smith (1959); Bryson & Gross (1961); Heilig (1967); Merritt (1968); Weynantes (1968); Gvozdeava *et al.* (1969, 1970); Meshkov (1970); Semenov, Syshchikova & Berezkina (1970); Law & Glass (1971); Pantazopol, Bellet & Soustre (1972); Henderson & Lozzi (1975); and Lozzi (1975). While most phenomena were found on plane surfaces, others have been found on curved surfaces; for example we have photographed a compound reflexion on a concave surface consisting of a regular reflexion followed closely by a Mach reflexion (figure 1*e*); we called it a regular Mach reflexion

0022–1120/79/4282-7310 $02.00

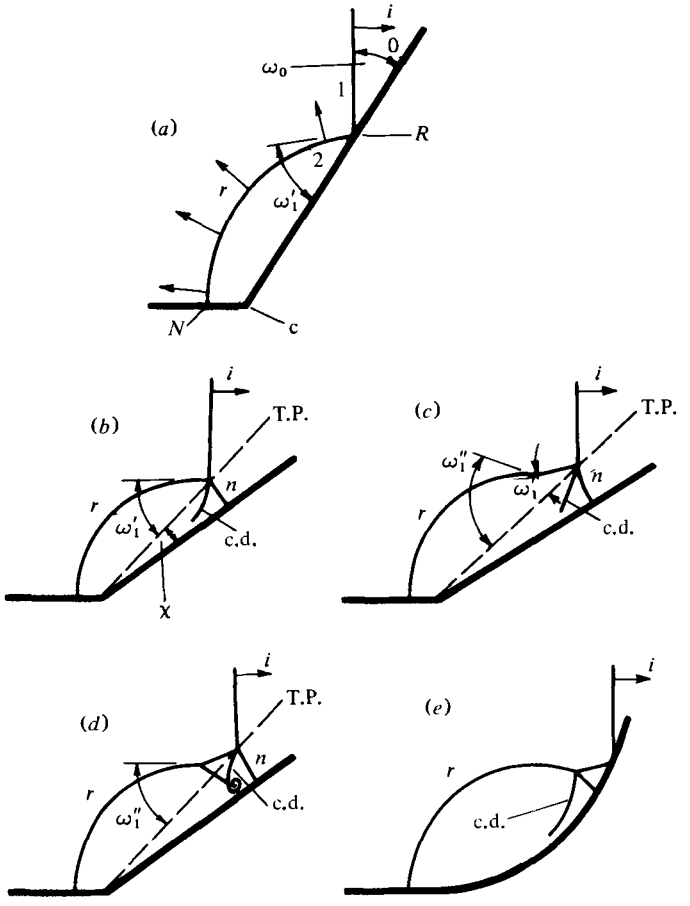

FIGURE 1. Diffraction wave patterns on a single corner. i, incident shock; r, reflected shock; n, Mach stem; c.d., contact discontinuity; ω_0, angle of incidence; ω_1', measured true angle of reflexion of r; ω_1'', wave angle of r at the kink; T.P., trajectory path; χ, trajectory path angle; c, corner. (*a*) RR, regular reflexion; (*b*) MR, Mach reflexion; (*c*) CMR, complex Mach reflexion; (*d*) DMR, double Mach reflexion; (*e*) RMR, regular Mach reflexion.

RMR. It will be assumed here that RR and MR are the fundamental systems and that the others are merely distortions and compounds of them.

Three criteria have been proposed for predicting transition between the two basic systems RR $\rightleftharpoons$ MR. They are conveniently discussed in terms of the angle of incidence ω_0 which i makes with the surface. Firstly there is the normal shock point $\omega_0 = \omega_N$, so called because the Mach stem is everywhere normal to the surface so that the streamline deflexion across it is zero $\delta_N = 0$. The Mach stem is presumed to be of zero length at transition and to grow rapidly to a visible length with $\omega_0 > \omega_N$.† The second criterion occurs when the flow downstream of r is sonic $M_2 = 1$, and $\omega_0 = \omega_0^*$ say. The third is when the streamline deflexion δ_1 across r is equal to the maximum value $\delta_1 = \delta_{1\max}$, for the Mach number M_1 upstream of r; it envisages transition as analogous to a shock detaching/attaching to a blunt body. The angle of incidence

† Experimenters often consider the appearance of the contact discontinuity to be a more sensitive indication of MR than the appearance of the Mach stem.

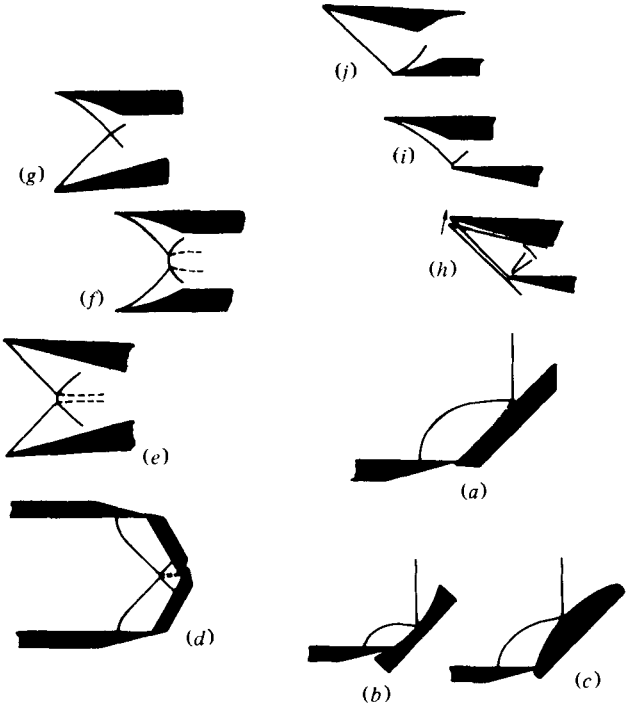

FIGURE 2. Illustration of the shock tube and wind tunnel models used to generate the shock wave systems for the experiments. (*a*) Single plane corner; (*b*) single concave surface corner; (*c*) single convex surface corner; (*d*) twin plane corners; (*e*) double wedges; (*f*) double concave wedges; (*g*) plane and concave wedges; (*h*) wedge and flat plate; (*i*) concave wedge and flat plate; (*j*) plane and concave wedge. Models (*a*)–(*d*) were used in the shock tube and the others in the wind tunnel.

at which it occurs is called the detachment or the extreme angle $\omega_0 = \omega_e$. The ordering of the criteria is $\omega_N < \omega_0^* < \omega_e$, but ω_0^* and ω_e are often so close together that it is impossible to resolve them by experiment, but usually ω_N can be easily resolved from the others.

Von Neumann (1963, p. 238) distinguished between strong and weak incident shocks, and he gave a rigorous definition of them in terms of a polynomial equation of eighth degree. Kawamura & Saito (1956) have given the same definition more conveniently in terms of shock polars, and for air with ratio of specific heats $\gamma = 1{\cdot}402$ the boundary between strong and weak i occurs at $\omega_0 = 41{\cdot}4°$ and at an inverse shock strength $\xi_i \equiv P_0/P_1 = 0{\cdot}433$, where $P_{0,1}$ are the pressures upstream and downstream of i respectively. Thus i is strong when $\xi_i < 0{\cdot}433$ and weak when $\xi_i > 0{\cdot}433$. He concluded that ω_N was the criterion for strong shocks and that ω_e was the one for weak shocks.

In our 1975 paper we presented wind tunnel and shock tube data for transition on single and twin shock generators which had plane, convex, or concave surfaces (figures 2*a–e* and *h*). Conditions were steady in the wind tunnel and unsteady in the shock tube. However, in the latter case the experiment could be subdivided into pseudo-stationary flows which had no length scale (they were self-similar), and flows which had a length scale but no stationary character (they were completely unsteady),

for example pseudo-stationary flow were produced by models (*a*) and (*d*) and non-stationary by models (*b*) and (*c*) (figure 2). We obtained the remarkably anomalous result that *strong shock transition occurred at the* ω_N *point for the stationary flows on models* (*e*, *h*), *also for the pseudo-stationary flow on model* (*d*), *and for the non-stationary flow on model* (*b*), *but that transition was delayed to values of* ω_0 *beyond the* ω_N *point and indeed beyond the* ω_e *point for the pseudo-stationary flow on model* (*a*), *and the non-stationary flow on model* (*c*). In explanation we suggested that the ω_N point was the correct criterion for all strong shock transitions and that the occasional anomalous persistence of RR beyond it was caused by the kink which obscured the true value of the reflected wave angle ω_1'. In other words it was only after ω_0 has become sufficiently larger than ω_N for the kink to be visible that we could measure ω_1', but for smaller ω_0 we were measuring the wave angle of the kink ω_1'' (figure 1*c*). Some evidence was presented to support the hypothesis because once the kink was visible both ω_1' and ω_1'' could be measured and it was found that ω_1' agreed with the theoretical value for MR, *while* ω_1'' *agreed with the theoretical value of* RR. No criterion was successful for weak shocks, although strangely the ω_N point predicted quite accurately the beginning of a discrepancy between the RR theory and the data, the same effect was noticed by White.

The purpose of the present paper is to report the results of further experiments on the transition phenomena. The idea was to put length scales into the flows so as to distort and magnify those parts which were of special interest. Two series of experiments supported the hypothesis about the ω_N point but another series in the wind tunnel caused us to modify it, because we obtained the extraordinary result that the transition RR$\rightleftharpoons$MR could be induced *almost anywhere* in the range $\omega_0 \leqslant \omega_N$, and it was even possible to suppress RR *completely*. Transition in these experiments were discontinuous and showed an interesting hysteresis effect. For weak shocks it was found that even the von Neumann theory of RR became progressively more inaccurate as the shocks became weaker. Real gas effects, particularly viscosity and the variation of specific heats, were considered but they could not adequately account for the observed phenomena.

2. Previous work

2.1. *Regular reflexion*

The von Neumann theory of RR is summarized by a single quadratic equation in the shock Mach number of r, and its coefficients are functions of the Mach number downstream of i. So there are either two real roots, a double root, or two complex roots. The real roots correspond to different strengths ξ_r of r and can be considered to be two solution branches, but the weaker branch usually appears in an experiment. The double root corresponds to the $\omega_0 = \omega_e$ point. The complex roots are not physically realistic and according to the theory RR is then impossible so it is plausible that in this event MR should appear. However when Bleakney & Taub (1949) and Griffith & Bleakney (1954) compared the theory with the experimental data of Smith (1945) they found that for diffraction over single plane corners RR persisted even when $\omega_0 > \omega_e$. In some cases the persistence amounted to about 5° greater than ω_e. These results were confirmed by Kawamura & Saito (1956) and Henderson & Lozzi. The effect was even more pronounced on convex surfaces (Heilig 1969; Henderson &

Lozzi 1975), but the later paper also showed that on concave surfaces the effect could be completely suppressed and transition promoted to the ω_N point.

The position is especially puzzling for weak shocks because the ω_N point is part of the *upper* branch solution and yet our 1975 experiments indicated that the data began to deviate from the lower branch solution once $\omega_0 > \omega_N$. Of course this may be mere coincidence but in the concave surface experiments the RR system jumped suddenly from the lower branch to the vicinity of the upper branch near the ω_N point although transition to MR did not occur until ω_0 was 2–3° larger.

2.2. *Mach reflexion*

Von Neumann only gave an outline of his theory of the three-wave confluence in MR, but it has been given in detail and extended since by Eggink (1943), Wuest (1948), Wecken (1949), Polachek & Seeger (1951), Guderley (1947, 1962), Sternberg (1959), Henderson (1964, 1965), Sakurai (1964), Mölder (1971), and others. Henderson (1964) showed that it was reducible to a polynomial equation of sixth degree with the pressure ratio of the Mach stem as the variable and the coefficients functions of $(\gamma, \omega_0, \xi_i)$. The number of roots of physical significance were shown to be either 0, 1, 2, or 3. The no-roots condition occurs only for weak shocks, yet experiment shows that MR nevertheless exists, so the theory appears to be wrong in this case. Guderley attempted to retrieve the position by introducing an expansion wave at the confluence, but Sternberg showed that the effect was probably undetectable on the laboratory scale. It has also been suggested that the effect could be explained by shock wave curvature (Mölder 1971), or by viscous effects (Sakurai 1964). The latter theory is considerably more accurate than the von Neumann theory especially when $\xi_i \geqslant 0{\cdot}9$, yet significant discrepancy still exists. However the von Neumann theory is accurate for strong shocks except for diffraction over single corners (figure 2*a*) near transition.

Summarizing, there are some important discrepancies between experiment and the von Neumann theory of RR and MR; these are:

(*a*) for weak shocks diffracting over single plane and convex surfaces RR is impossible when $\omega_0 > \omega_e$ because there are no physically realistic solutions;

(*b*) for weak shocks, MR frequently appears even though according to the theory it is impossible, again because there are no physically realistic solutions, and when the theory does provide solutions there is often a large discrepancy between them and the data;

(*c*) for strong shocks diffracting over single plane corners and convex surfaces the theory is inaccurate near transition, but it is accurate elsewhere for these and other surfaces.

These discrepancies may be collectively referred to as the von Neumann paradox.

2.3. *Flow classification*

The necessary conditions for the existence of any phenomenon are determined theoretically by ranges of values of the parameters $(\gamma, \omega_0, \xi_i)$, or for a given gas (ω_0, ξ_i). Here it is convenient to use the equivalent set (ω_0, M_0), where $M_0 = M_1/\sin\omega_0$ is the free-stream Mach number onto i, and $M_i(\xi_i)$ is the shock Mach number of i. The classification scheme for these conditions is as follows and is illustrated in the polar diagrams of figure 3.

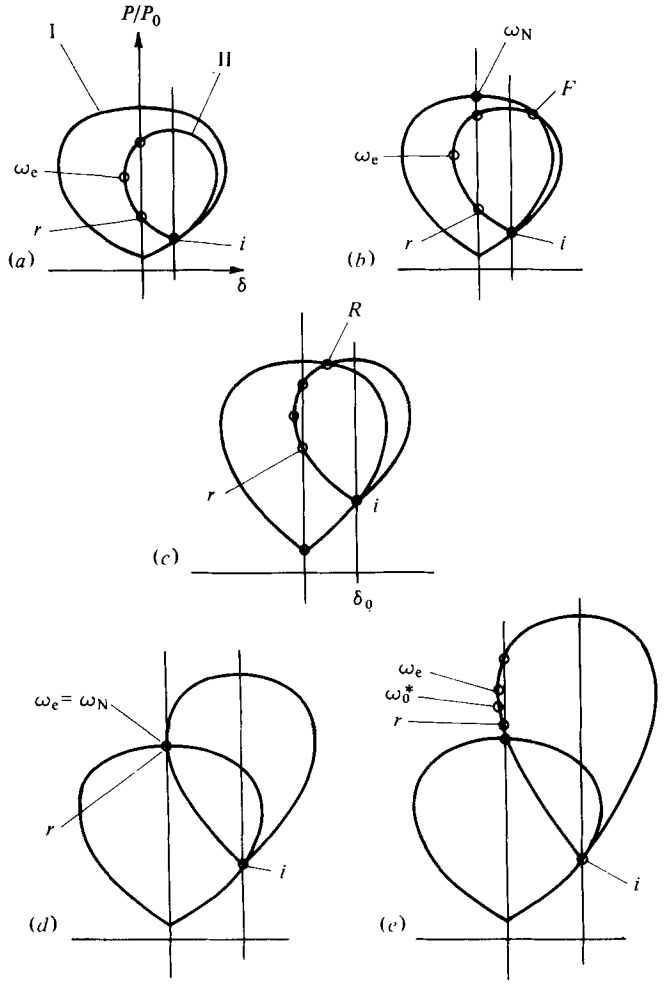

FIGURE 3. Polar geometry for different regimes of incident free-stream Mach number (M_0). (*a*) $M_0 < 1{\cdot}25$; (*b*) $1{\cdot}25 < M_0 < 1{\cdot}48$; (*c*) $1{\cdot}48 < M_0 < 2{\cdot}23$; (*d*) $M_0 = 2{\cdot}23$; (*e*) $M_0 > 2{\cdot}40$. I, M_0 polar; II, M_1 polar; F, reflected shock r inclined forward, same family as i; R, r inclined backwards, opposite family to i.

(*a*) $M_0 < 1{\cdot}25$. There are no physically realistic solutions for MR in this range for any (ω_0, M_0). When $M_0 > 1{\cdot}25$ the same thing happens for a restricted range of ω_0 but this shrinks rapidly with increasing M_0 (Henderson 1964).

(*b*) $1{\cdot}25 < M_0 < 1{\cdot}48$. Solutions for MR exist for some ω_0 and when they do r is inclined forwards at the confluence, which means that i and r are in the same family in the sense that two characteristics are in the same family.

(*c*) $1{\cdot}48 < M_0 < 2{\cdot}23$. Solutions for MR also exist for some ω_0 but r is now inclined backwards at the confluence (other family), but at larger ω_0 it may again incline forwards.

(*d*) $M_0 = 2{\cdot}23$. This is the boundary between strong and weak shocks.

(*e*) $M_0 = 2{\cdot}40$. The flow downstream of r is sonic, $M_2 = 1$.

(*f*) $M_0 > 2{\cdot}40$. The flow downstream of r is supersonic, $M_2 > 1$ (Henderson 1965) and MR is more likely to be replaced by DMR, especially with increasing M_0.

Although these conditions are necessary for the existence of a particular wave system they are not sufficient because the boundary conditions are also important. Indeed the purpose of this paper could be expressed alternatively as an investigation of the different boundary conditions with given (ω_0, M_0).

3. Experiments

3.1. *Models and methods of measurement*

The models are illustrated in figure 2; those for the shock tube were either single corners with plane or curved surfaces (figures 2*a–c*), or a twin corner model with plane surfaces (figure 2*d*). Each wind tunnel model (figures 2*e–j*) consisted of two parts: one was a wedge with either a plane or concave surface and the other was either another wedge or a flat plate.

A schlieren system was used for all the experiments; it was made by Carl Zeiss and the aperture of its mirrors was 20 cm and both were off-axis parabolic accurate to better than 0·1 wavelengths. The light source was a $\frac{1}{4}$ μs flash from an argon jet stabilized arc. The camera was a modified Haselblad with 80 and 250 mm lenses. Photographic negatives obtained with this equipment were displayed on a Nikon profile projector and enlarged by a factor of about 10. While the projector could measure better than 1 min of angle the resolution of our photographs did not permit measurements of ω_0, ω_1' and, ω_1'', to better than about 6 min. After a model had been set up its geometry was measured by a cathetometer with a Nikon goniometer eyepiece accurate to about 10 min. In the shock tube the speed of the incident shock was measured with three Atlantic Research Corp LC71 piezo-electric transducers spaced about 50 cm apart. Microsecond counters determined the time between the transducers to the nearest μs and gave four significant figures, and the spacing was known to the same number of figures. From these measurements and the initial temperature of the gas we could calculate the shock Mach number M_i of i, and then ξ_i. For the wind tunnel M_0 was known by calibration.

3.2. *The shock tube experiments*

3.2.1. *Strong shocks on concave surfaces.* In our 1975 shock tube experiments with single corners we used a plane surface (figure 2*a*), a convex surface (figure 2*c*) of radius $R = 13{\cdot}0$ cm, and a concave surface (figure 2*b*) of radius $R = 7{\cdot}27$ cm.† For strong shocks at $M_0 = 4{\cdot}0$ on the concave model transition took place at the ω_N point but persisted beyond the ω_e point for the other models. It was plausible therefore that the ω_N point should remain valid up to some limiting value of R in the range

$$7{\cdot}25 < R < \infty \text{ cm}.$$

Although it was impracticable to determine R_{limit} it was decided to experiment with a larger radius model and $R = 19$ cm was selected.

Another important boundary parameter is the initial plate incident angle θ_i (figure 4) which determines the incidence $\omega_0 = \omega_i$ at which i first encounters the curved

† These radii were quoted wrongly in our 1975 paper as 20 cm and 15 cm respectively.

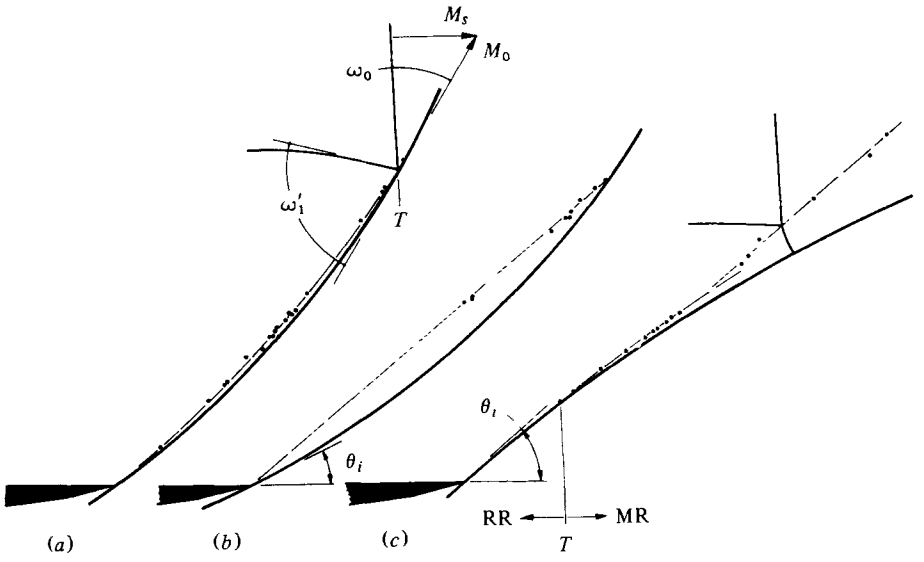

FIGURE 4. Measurements on some trajectory paths of Mach reflexion confluences on curved surfaces at $M_0 = 4{\cdot}0$. θ_i, initial plate incidence angle; M_s, shock Mach number of i; M_0, free-stream Mach number of i. (*a*) concave surface model (*b*) (figure 2) with radius $R = 7{\cdot}25$ cm, $\theta_i = 36°$, $\omega_i = 54°$; (*b*) Model (*b*) with $\theta_i = 28°$, $\omega_i = 62°$; (*c*) convex surface model (*c*) (figure 2) with radius $R = 13$ cm, $\theta_i = 45°$, $\omega_i = 45°$.

surface. When the initial reflexion is regular then $\omega_i = \frac{1}{2}\pi - \theta_i$. The effect of two different values of θ_i on the trajectory path of the MR confluence is shown in figures 4(*a*, *b*) for the 7·25 cm surface. In all of our experiments with curved surfaces we plotted curves of this type and measured ω_0, ω_1' and ω_1'' which respect to them. In figure 4(*a*), $\theta_i = 36°$, $\omega_i = 54°$, and ω_0 is never very far from the $\omega_N = 33{\cdot}4°$ point and the Mach stem is therefore always short and the trajectory path is close to the surface. This suggests that if the surface was much flatter then the Mach stem might become too short to be observable. In figure 4(*b*) $\theta_i = 28°$, $\omega_i = 62°$, and ω_0 departs rather more from ω_N and the trajectory path now makes a straight line across the surface and does not attempt to follow it. The Mach stem changes its length continuously to bridge the gap between the line and the surface. Both effects are found consecutively on a convex surface (figure 4*c*), where the trajectory path initially hugs the surface and later 'separates' from it to form a straight line.

Further data for a concave surface with $M_0 = 4{\cdot}0$ is presented in figure 5 to explore the effects of increasing R to 19 cm and on changing θ_i. In figure 5(*a*) it will be noticed that transition persists *apparently* to the ω_e point with $\theta_i = 51°$, $\omega_i = 39°$, but that in figure 5(*b*) transition occurs *at* the ω_N point with $\theta_i = 47°$, $\omega_i = 43°$. To offer an explanation for this surprising result we begin by remarking that the trajectory paths of figures 5(*a*, *b*) are qualitatively the same as those shown in figures 4(*a*, *b*) respectively, so the Mach stem will be generally shorter and harder to observe† in the $\theta_i = 51°$ experiments than in the $\theta_i = 47°$ ones. Furthermore in figure 5(*b*) with $\omega_0 > \omega_N$ the wave system is mostly, but not always, observed to be a DMR with a well-defined kink in its reflected shock r. We measured the kink wave angle ω_1'' as well

† The contact discontinuity will also be harder to observe.

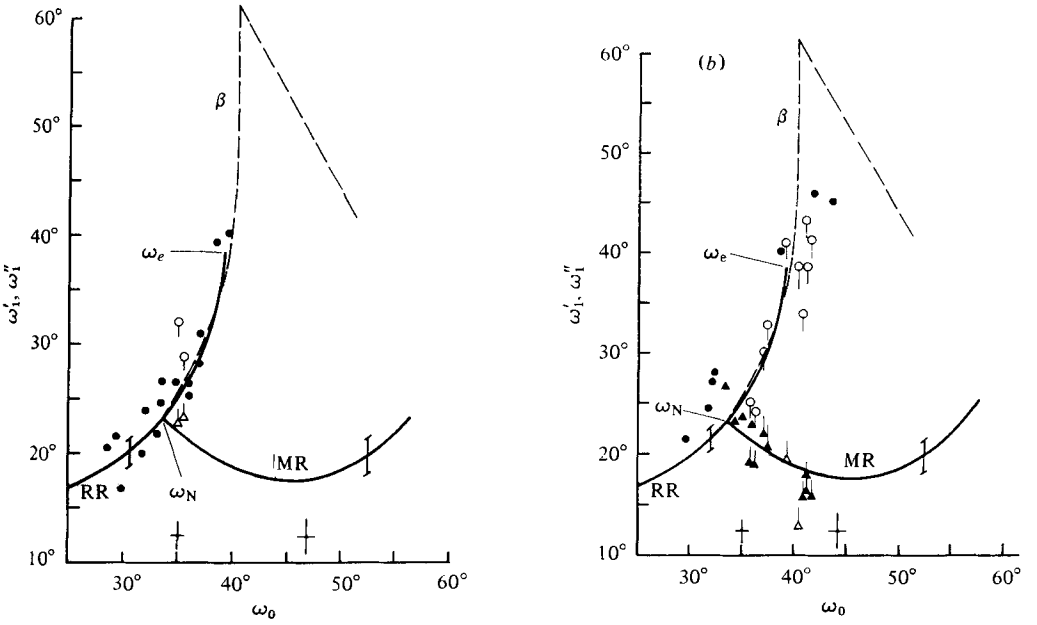

FIGURE 5. Shock tube experimental data for plane shocks diffracting over a single concave corner (see figure 2*b*) with surface radius 19 cm and $M_0 = 4{\cdot}0 \pm 0{\cdot}02$. Reynolds number based upon radius is $1{\cdot}5 \pm 0{\cdot}5 \times 10^6$. (*a*) Initial wave incidence angle $\theta_i = 51{\cdot}0 \pm 0{\cdot}5°$, $\omega_i = 39{\cdot}0 \pm 0{\cdot}5°$; (*b*) $\theta_i = 47{\cdot}0 \pm 0{\cdot}5°$, $\omega_i = 43{\cdot}0 \pm 0{\cdot}5°$. ●, RR experimental data point; ○, experimental data point with unresolved details at confluence and/or if a kink in the reflected wave *r* is present then this represents the angle at the kink; △, experimental data point, doubtful Mach reflexion and reflected wave angle before the kink; ▲, experimental data point with distinct Mach stem and/or contact discontinuity visible; ○, △, when *r* has a kink then the two angles ω_1' and ω_1'' as thus shown; ——, curves for RR and MR from inviscid von Neumann theory; – – –, β, theoretical curve calculated from polar diagrams similar to those shown in figure 6; I, uncertainty caused by variation in M_0; +, magnitude of experimental error.

as the true wave angle ω_1' and as shown in figure 5(*b*) the ω_1' data agrees well with the MR theory but the ω_1'' data agrees with the RR theory. This suggests that the famous persistence of RR beyond the ω_N point is *spurious* and that what experimenters including ourselves have been measuring is the *kink wave angle* ω_1'' and not the *true wave angle* ω_1' which is sometimes unresolvable. In fact inspection of figure 5(*b*) shows that for $\omega_0 > \omega_N$ there are three apparent RR and three MR data points appearing among the more numerous DMR points, while in figure 5(*a*) there are two DMR points appearing among the apparent RR points. Hence by experiment we have, for DMR,

$$\omega''_{1\,\text{experiment}} \approx \omega'_{1\,\text{RR theory}}. \tag{1}$$

Referring to figure 6, the upstream Mach reflexion in DMR deflects the flow towards the surface but the boundary condition requires the flow to be brought back parallel to the surface. Now if this occurs in a region which is too small for the Mach reflexion to be observable then both RR and DMR should have very nearly the same apparent wave angle of *r*. The polar diagram was constructed on the assumption that the downstream Mach reflexion in the DMR brought the flow back parallel to the surface. The result is that the RR solution α is practically indistinguishable from the DMR

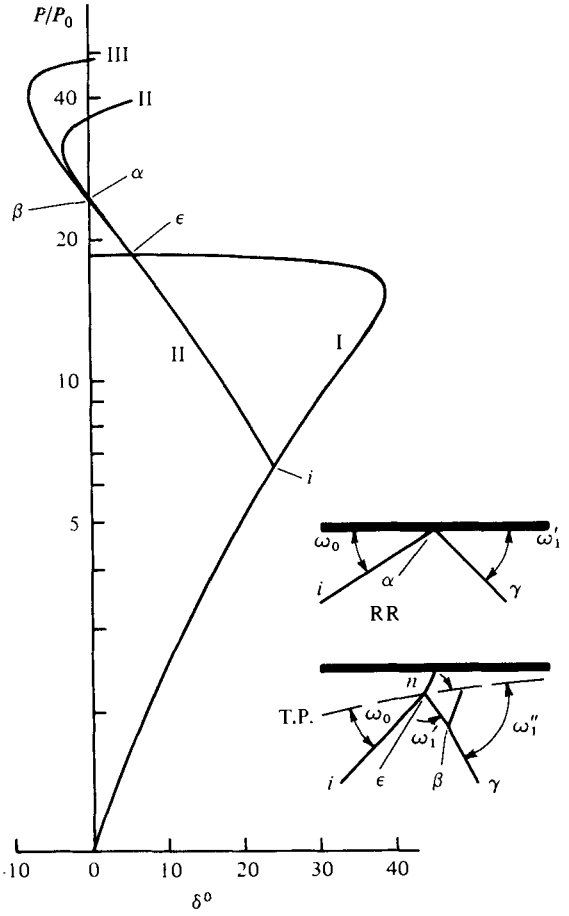

FIGURE 6. Polar diagrams for regular RR and double Mach DMR reflexion, for $M_0 = 4{\cdot}0$, $\gamma = 1{\cdot}402$, and $\omega_0 = 37{\cdot}0°$. I, M_0 4·0 polar; II, $M_1 = 2{\cdot}29$ polar for flow downstream of i; its intersection with the ordinate axis defines the RR solution α; III, $M_2 = 1{\cdot}55$ polar; its intersection β defines the DMR solution. For other symbols see the captions to figures 1, 3 and 4.

solution β, for $M_0 = 4{\cdot}0$, and $\omega_0 = 37{\cdot}0 > \omega_N$, so that $\omega'_{1\,RR} \approx \omega''_{1\,DMR}$. The broken curve labelled β in figure 5 was computed in this way, and it is seen how it is negligibly different from equation (1) for $\omega_0 < \omega_e$. Further evidence is provided by figures 7, 8 and 9 (plates 1 and 2). In figure 7 there is a DMR and although the kink is only slight its associated Mach stem is distinctly visible on the original plate. This experiment was with the $R = 7{\cdot}25$ cm model and it was within the range $\omega_N < \omega_0 < \omega_e$. In figure 8 R has been increased to 19 cm but the other conditions are nearly the same as in figure 7. There is now an apparent RR *with a kink* and incidentally such a wave system has not been reported before; however, it is almost certainly an unobservable DMR because if we increase the time delay of our photography to allow the wave system more time to grow then we obtain the result shown in figure 9, which is plainly a DMR.† All of which supports the hypothesis that the persistence of RR for $\omega_0 < \omega_N$ is spurious.

† Note that ω_0 only changes by 0·7° between figures 8 and 9 and that $\omega_N < \omega_0 < \omega_e$, so the change in ω_0 is not enough to invalidate the conclusion.

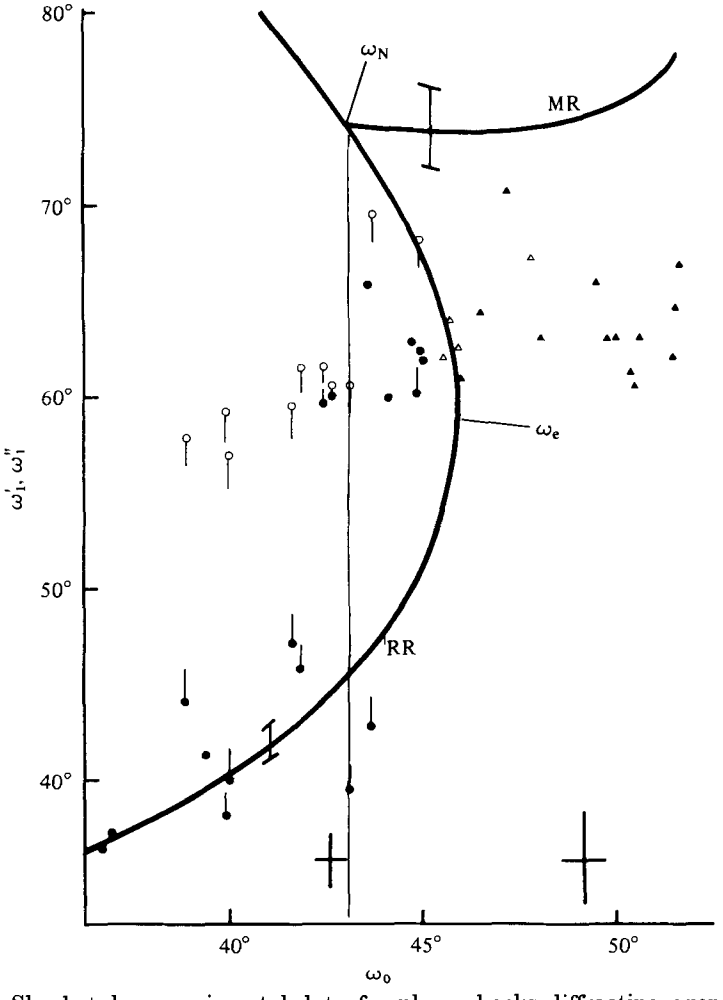

FIGURE 11. Shock tube experimental data for plane shocks diffracting over a single concave corner (figure 2*b*) with surface radius $R = 7{\cdot}25$ cm and $M_0 = 1{\cdot}7 \pm 0{\cdot}1$, Reynolds number at transition based upon radius 1×10^6. For symbols see caption to figure 5.

3.2.2. *Weak shocks on concave surfaces.* Data was presented in the 1975 paper for weak M_0 1·7 shocks on the 7·25 cm concave surface. It was during these experiments that the RMR system, figure 10 (plate 2), was first photographed. The kink was there associated with an MR which formed downstream of the primary RR. Further and more detailed measurements have now been made of the wave angle of r both at the kink ω_1'' and at the primary reflexion ω_1', and the results are shown in figure 11. As with all of our experiments with curved surfaces the data has a fair amount of scatter due to the difficulty of photographing the wave system precisely at the instant when $M_0 = 1{\cdot}7$.

For $\omega_0 < 43°$, the agreement between the lower branch of the RR theory and the ω_1' data is probably satisfactory given the reason for the scatter, but everywhere else the theory seems to fail. At $\omega_0 \approx 43°$ the data exhibits a sudden jump and thereafter it corresponds roughly to the upper branch solution of RR. The smallest ω_0 for

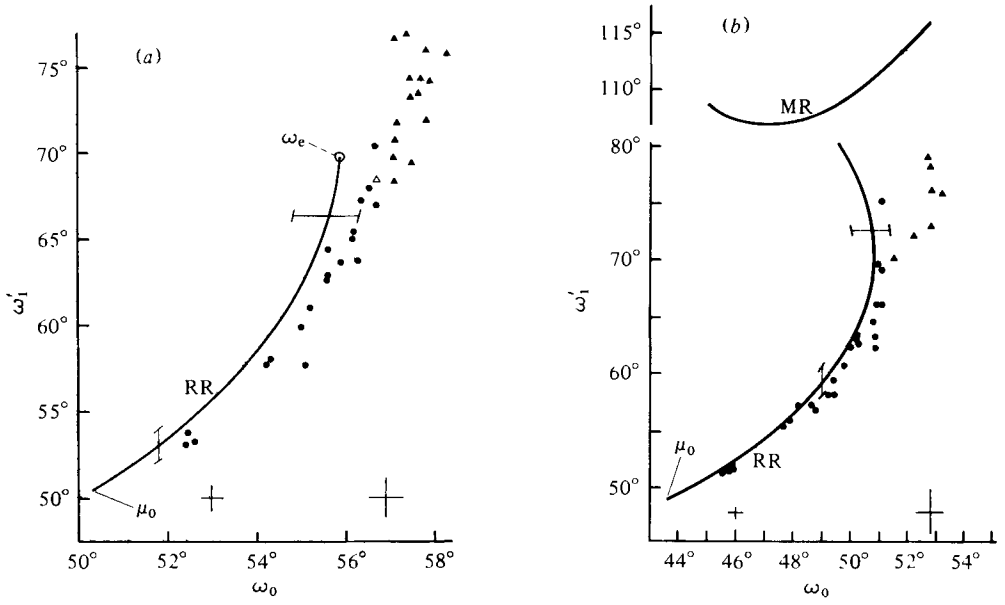

FIGURE 12. Shock tube experimental data for plane shocks diffracting over a twin plane corner model (figure 2*d*). (*a*) $M_0 = 1{\cdot}3 \pm 0{\cdot}02$, Reynolds number based on radius $9{\cdot}0 \pm 2{\cdot}0 \times 10^6$; (*b*) $M_0 = 1{\cdot}45 \pm 0{\cdot}02$, Reynolds number based on radius $1{\cdot}0 \pm 0{\cdot}2 \times 10^6$, μ_0 Mach angle for M_0; for other symbols see caption to figure 5.

which a kink was observed was $\omega_0 \approx 39°$ but unlike strong shocks there is no adequate theory for ω_1'' at the kink. The ω_N point is now on the upper branch of the RR curve and perhaps it is associated with the discontinuity but the data is not definite about this. White suggested that weak shock transition may be associated with the ω_N point but the present data does not support this hypothesis. Actually the ω_e point is closest to transition but not too much credence can be attached to this because the ω_1' data is 3 to 4° above the ω_e point. Following transition, the theory does give an MR solution, but it fails to agree with the data, so for these experiments the theory is in a very unsatisfactory state. Possibly the most interesting result is the sudden jump in ω_1' at $\omega_0 \approx 43°$ and presumably this must also be associated with a sudden jump in the surface pressure, and if so this could be of technical importance.

3.2.3. *Very weak shocks on twin symmetrical plane surfaces.* For weak shocks we had noticed in the 1975 experiments that the data began to deviate from the theory as transition was approached. The discrepancy increased continuously for single plane and convex corners, but for concave corners it was a discontinuity as we have just seen (figure 11). The data of other experimenters were also inspected and there were signs of a continuous discrepancy for the $\xi_i = 0{\cdot}9$ data of Griffith & Bleakney (1954) on single plane corners but no sign of it in the $\xi_i = 0{\cdot}8$ data of Bleakney & Taub (1949), or Kawamura & Saito (1956) on the same type of corner, nor in the $\xi_i = 0{\cdot}915$ data on the twin corners of Smith (1959). It was decided to explore the matter further by obtaining data for the very weak shocks corresponding to the polar diagrams in figures 3(*a*, *b*). In order to minimize the effects of viscosity a symmetrical twin corner model was used, figure 2(*d*).

The data presented in figure 12(*a*) for $M_0 = 1{\cdot}3$ is representative of figure 3(*a*), even

though $M_0 > 1{\cdot}25$. The reason (Henderson 1964) is that for $M_0 = 1{\cdot}3$ the region where the theory has no physically realistic MR solutions occurs when $\omega_0 > 54°$ (corresponds to $\delta_0 = 2{\cdot}4°$), and nearly all of the data meets this condition. The shock strength range is $0{\cdot}93 < \xi_i < 0{\cdot}80$. Evidently there is a discrepancy between the theory and the data for the entire RR range, while for the MR range there are of course no useful solutions. It will be noticed that transition takes place about 1° beyond the ω_e point. In figure 12(*b*) the data is for $M_0 = 1{\cdot}45$, $0{\cdot}94 < \xi_i < 0{\cdot}70$ and is typical of the polar diagram figure 3(*b*). The same effects are present but they are not so pronounced. The theory now provides a solution for MR but it does not agree with the data.

Thus for the regular reflexion of weak shocks there may be a new effect here, namely, *there is an increasing discrepancy between the von Neumann theory and the data as* (ξ_i, ω_0) *increases*. It seems unlikely that the effect can be viscous phenomena, because the symmetry of the model should practically prevent the formation of a contact discontinuity and with it most of the viscous influence. Also for weak Mach reflexions the Sakurai (1964) viscous theory itself has discrepancies although it is a significant improvement on the von Neumann theory. Finally the effect of variation of specific heats is slight for these weak shocks, so at present there is no satisfactory explanation of the discrepancies.

3.3. *Wind tunnel experiments*

3.3.1. *The models.* The tunnel Mach number was fixed at M_0 2·95, which essentially restricted our experiments to strong shocks. One objective was to reproduce some of the effects found in the shock tube, particularly to see if a kink could be generated, and another was to explore the effect of scale on transition by using models with curved surfaces. During the work some unexpected phenomena appeared and the opportunity was taken to study them as well.

None of the models in figures 2(*e*)–(*j*) spanned the tunnel; this was to avoid the troublesome interaction of the shock waves with the boundary layers on the side walls of the tunnel. Viscous effects were also reduced in models (*e*), (*f*) and (*g*), by making each from two wedge-like bodies arranged so that the shocks i_1, i_2 which they generated interacted well away from their surfaces. For models 2*h*, *i*, and *j*, viscous effects were reduced by causing the incident shock *i* to impinge on the tip of the lower plate, where the local boundary layer would be thin.† All of the models formed an internal converging passageway which terminated in a throat at the downstream end, and caused them to behave like small supersonic diffusers. In fact in all of these experiments we encountered a 'starting' phenomenon associated with establishing the wave system inside a model. Now because a model did not span the tunnel completely air could be ejected from it sideways, particularly near its throat, and this stabilized the internal wave system for a useful range of wave incidence angles ω_{01}, ω_{02} of i_1 and i_2, or ω_0 of *i*. These wave angles were measured at the confluences and were varied by changing the model geometry. For example to increase $\omega_{01,02}$ for the model in figure 2(*f*) it is necessary only to increase the distance between its two parts while keeping them parallel. This permits more compression waves from the concave

† More precisely this reduced the scale of the viscous phenomena and helped confine its main effects to a small region, and the shocks should therefore have approached their inviscid behaviour near the region.

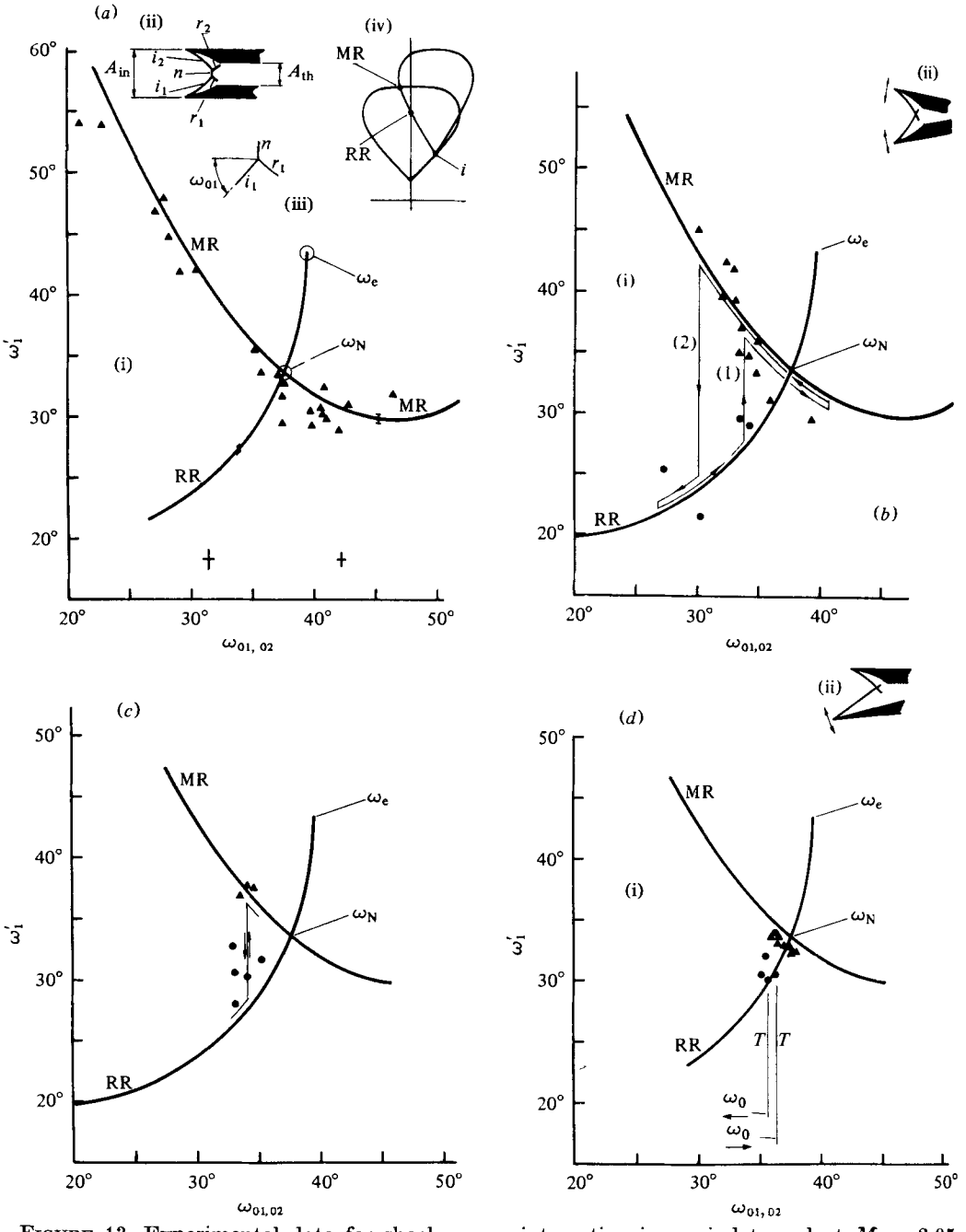

FIGURE 13. Experimental data for shock waves interacting in a wind tunnel at $M_0 = 2{\cdot}95$. (*a*) Model (*f*) of figure 2, radius of concave surfaces 10 cm, chordal distance across surfaces 4·2 cm; the two parts of the model were always parallel between 4·5 and 6·5 cm apart, diagram (ii); (*b*) same model as for (*a*) but now one part is rotated with respect to other, nominal distance apart initially 4 cm, diagram (ii); (*c*) same as for (*c*) but now the nominal initial distance apart increased to 5·4 cm; (*d*) model (*g*) (figure 2) with a plane wedge and with a concave wedge which has been modified by partly grinding off its shoulder; the parts were rotated as in (*b*). i_1, i_2, incident shocks; n, Mach stem; r_1, r_2, reflected shocks; A_{in} cross-sectional area of inlet; A_{th} cross-sectional area of throat including allowance for gaps between model and tunnel walls; ω_{01}, ω_{02}, angles of incidence of i_1 and i_2 measured at the confluences and with respect to the tunnel centre-line. For other symbols see caption to figure 5.

surfaces to overtake $i_{1,2}$ before they reach their confluences and thus cause them to steepen and to increase $\omega_{01,02}$. Alternatively the two parts of the model could be rotated with respect to each other. We used both methods.

3.3.2. *Suppression and promotion of transition.* The model (f) of figure 2 had symmetrical concave surfaces of radius $R = 10$ cm, and the chordal distance across each surface was 4·2 cm. For this series the two parts were always parallel and the distance between them varied from 4·5 to 6·5 cm so as to vary $\omega_{01,02}$, but the geometry was not altered while the tunnel was running. The lowest limits on $\omega_{01,02}$ were determined either by the shock system oscillating – intake buzz – or by the wave system being expelled from the model due to it becoming unstarted. At the upper end of the range the experiments were terminated about 6° beyond the ω_e point. The data is presented in figure 13(a) and there is the striking result that RR and transition have been completely suppressed over the *entire range* of $\omega_{01,02}$. To the best of our knowledge RR has always appeared in all previous experiments when $\omega_0 < \omega_N$. The MR theory predicts that the Mach stem is convex forward to the oncoming flow for $\omega_0 < \omega_N$, so the contact discontinuities are deflected away from the centre-line at the confluences. These effects were observed and an example of them may be inspected in figure 14 (plate 3) where $\omega_{01} = \omega_{02} = 30{\cdot}8°$. We formed the hypothesis that RR had been suppressed because the model was always partly unstarted, that is RR would occur in the started state and MR in the partly unstarted state. Now a supersonic diffuser can be started by sufficiently reducing its area ratio A_{in}/A_{th} (Henderson 1967), where A_{in} is the cross-sectional area at inlet and A_{th} at the throat.† In the next series we tried this.

The same model was used but now its two parts were set nominally 4 cm apart, which corresponded to particular slots in the sting mounts. The lower part was set at a fixed angle to the centre-line which by experience was known to give a desired $\omega_{01} \approx 33°$ say. The upper part could be rotated while the tunnel was running and it was set initially at a larger angle so as to open the model throat widely and facilitate starting. Then with the tunnel running the upper part was rotated downwards to make the model symmetrical, and measurements taken, figure 13(b). At first with $\omega_0 < \omega_N$ we observed an RR system but, if the upper part was rotated downwards a little further so that the model became unsymmetrical, then the wave system jumped discontinuously to an MR system which persisted *even* if subsequently the upper part was returned to its symmetrical position, or indeed some way beyond it. Thus we found a hysteresis effect and it is marked by pathway (1) in figure 13(b); the associated discontinuous transition is denoted here by RR ⌐→ MR. As a further demonstration the upper part was rotated still more away from the centre-line with stops on the way for measurements, until a discontinuous transition to RR was observed MR ⌐→ RR; it is marked by pathway (2), and completes a cycle. The discontinuous transitions and the hysteresis are of course strong evidence that the starting hypothesis is correct.

In the next series the two parts were separated to a nominal 5·4 cm and the experiments repeated (figure 13c). The hysteresis effect has now been reduced to a negligible amount and the transition has been shifted towards the ω_N point. The magnitude of

† The throat area A_{th} is not well defined because the model does not completely span the tunnel. A_{th} must include an allowance for the gaps between the model and the tunnel walls; it is essentially the cross-sectional area of the sonic surface where the flow chokes.

the discontinuity may be defined to be the difference in ω_1' between RR and MR at transition, and it will be seen that it has been reduced. In an attempt to suppress the starting effects completely we adopted the rather drastic procedure of replacing one of the concave parts by a plane one and partly grinding off the shoulder of the other (figure 2*g*). Transition now took place near the ω_N point (figure 13*d*), but a small amount of hysteresis was detectable. Our 1975 experiments with plane surface model (*e*) of figure 2 can be regarded as part of the present study, and for them transition took place continuously at the ω_N point without any hysteresis, figure 4(*b*) of Henderson & Lozzi (1975).† It is now asserted that the starting shock is the Mach stem n (figure 13*a*) and that it interacts with the incident shocks $i_{1,2}$ to produce the shocks $r_{1,2}$ and that these can also be considered as part of the starting shock ($r_1 n r_2$). An example of it is shown in figure 14 (plate 3).

It is concluded that transition between RR and MR can be promoted or suppressed anywhere in the range $\omega_0 \leqslant \omega_N$ by a suitable choice of the downstream boundary conditions, and particularly by the effective area ratio A_{in}/A_{th}. However for $\omega_0 < \omega_N$ transition is associated with hysteresis and is discontinuous and if it is desired to promote or suppress it at a given ω_0 then it is also necessary to specify the direction RR⌐→MR, or MR¬↳ RR.

3.3.3. *The failure to promote* RR *for* $\omega_0 > \omega_N$, *and the promotion of a kink.* In this series we tried to promote RR and transition beyond the ω_N point $\omega_0 > \omega_N$. The model is shown in figure 2(*h*) and consisted of a plane movable wedge and a flat plate. Initially the wedge was set so that i just missed the leading edge of the plate. Now i deflects the streamlines downwards through the angle $-\delta_0^\circ$ say, and causes the plate to be at incidence, but the plate must bring the flow back parallel to itself and it deflects the flow through the same angle but in the opposite direction $+\delta^\circ$. Consequently there will be an oblique shock r on the plate leading edge and the wave angle ω_1' of r should be exactly the same as if i had produced r by direct reflexion off the plate. Now suppose the wedge rotates slightly until i intersects the plate leading edge, then if this is done with $\omega_0 > \omega_N$ we shall be trying to promote RR by bringing together the i and r shocks corresponding to a particular RR solution. To maximize our chances of success we chose ω_0 to be in the range $\omega_N < \omega_0 < \omega_e$. It did not work, for the moment that i touched the plate a Mach stem became visible, and there was a corresponding and sudden reduction in ω_1'. The results are shown in figure 15(*a*) and it is clear that once again ω_N is the transition point. For some experiments there were slight signs of a kink, a CMR, and three measurements of ω_1'' are included. While the effect was slight it did encourage us to try and promote a more definite effect.

In the first attempt the plane wedge was replaced by a concave one (figure 2*i*), but this suppressed RR completely with results similar to those shown in figure 13(*a*); the data are omitted because they show nothing new. In the next attempt we returned to the plane wedge but replaced the flat plate by a concave surface (figure 2*j*). In this case, we appear to have obtained a CMR (figure 15*b*), but the effect is weak, the maximum difference between ω_1' and ω_1'' that we measured was only about 5°. We measured ω_1'' at the maximum slope, that is at the inflexion point, of r. While the data in figure 15(*b*) seems definite enough it should perhaps be accepted with some reserve, especially when one inspects figure 16 (plate 3) which shows how slight is the forward

† The Mach number was slightly smaller, $M_0 = 2{\cdot}85$, in Henderson & Lozzi (1975).

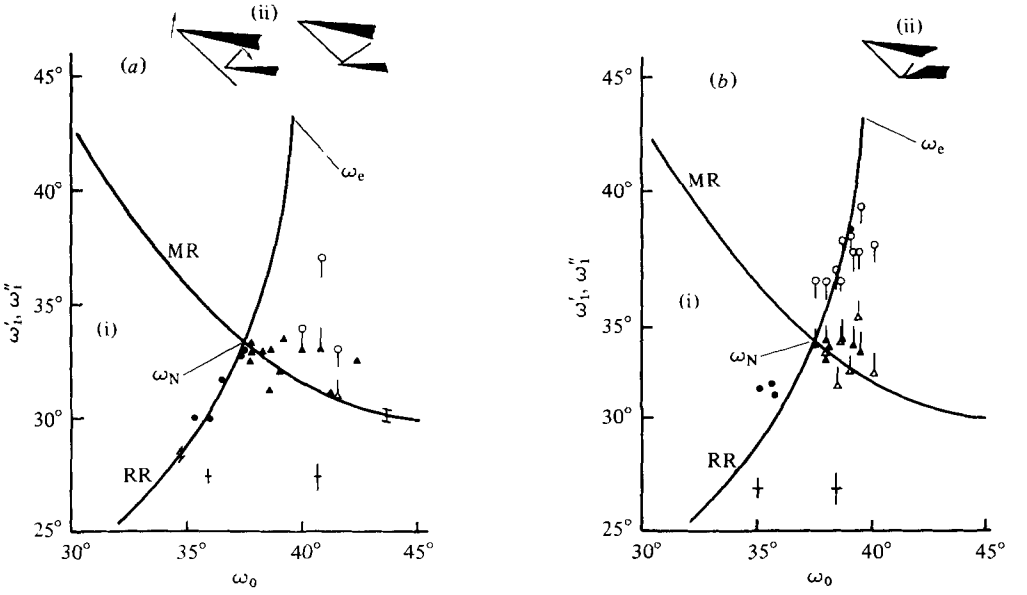

FIGURE 15. Experimental data for a shock wave interacting with the leading edge of a plate at M_0 2·95 ± 0·05. Initially the incident shock i just missed the leading edge of the plate, inducing incidence of the plate and generating the shock r, then with the tunnel running the wedge was rotated slightly until i intersected the leading edge of the plate. (*a*) Model (*h*), (*b*) model (*j*) (see figure 2). For other symbols see caption to figure 5.

concavity of r. Nevertheless the wave angle ω_1'' measured at the kink *agrees quite well* with the theoretical angle ω_1' of the RR solution, so once more equation (1) is satisfied. So it seems that we have observed a CMR not only for the non-stationary, and pseudo-stationary flows in a shock tube but also for the stationary flow in a wind tunnel. In figure 15(*b*), ω_1' agrees quite well with the MR solution. Now the Mach stem was always very short in this series 0·1 cm or less in length, so if our schlieren system had been unable to resolve it, and a glance at figure 15(*b*) shows that this did happen on one occasion, then we would have concluded wrongly that RR had persisted beyond the ω_1 point.

4. Conclusion and remarks

(*a*) For strong shock waves reflecting off solid surfaces or intersecting with each other, transition from regular RR to irregular (MR, CMR, DMR) reflexion, or vice versa, takes place continuously through the ω_N point, that is where the Mach stem while of vanishingly short length is everywhere normal to the flow. But if the disturbances which generate the shocks (for example solid surfaces) form a downstream throat then, by adjusting A_{in}/A_{th}, transition may be promoted or suppressed anywhere in the range $\omega_0 \leqslant \omega_N$, and it is even possible to suppress RR completely. Transition is then a starting–unstarting phenomenon which is discontinuous and associated with hysteresis with respect to direction.

(*b*) For strong shock waves diffracting over single plane corners where the flow is pseudo-stationary, or a single corner with a curved surface where it is non-stationary,

it is often reported that RR and transition persist beyond the ω_N point, but the effect is spurious. It is due firstly to the Mach stem being too small to be observable so that the irregular system has the appearance of a regular one. The measurable wave angle of the reflected shock is then at the kink and because the boundary condition requires the flow to be parallel to the surface this forces the kink wave angle ω_1'' to be negligibly different from the theoretical wave angle ω_1' of RR. Measurements of ω_1'' for CMR and DMR are shown in figures 5(*b*) and 15(*b*) and they agree quite well with the *theoretical* value of ω_1' of the RR solution, which demonstrates the deceptive nature of the effect as do figures 8 and 9 (plates 1 and 2).

(*c*) For weak shocks waves it was known previously that the von Neumann theory of Mach reflexion was either a partial or a complete failure, but experimental evidence presented here, figures 11 and 12, indicates that even the theory of regular reflexion becomes increasingly inaccurate as the shocks become progressively weaker.

(*d*) For weak shock waves, the transition criterion is unknown.

(*e*) For weak shock waves diffracting over single corners with concave surfaces a discontinuity was observed in the regular reflexion range, figure 11, during which the wave system jumped from the lower branch solution of RR to a position corresponding roughly to the upper branch, or vice versa. The data agrees well with the lower branch but not for the upper branch. The discontinuity does not seem to be associated with transition to Mach reflexion. The theory of this diffraction is in an unsatisfactory state.

The von Neumann theory is based on assumptions which include those of a perfect gas; so the gas is supposed to be inviscid and have constant specific heats. Now the variation of specific heats is too small an effect to explain the discrepancies found with weak shocks, and as we have seen the Sakurai viscous theory of weak Mach reflexion also has significant discrepancies. For strong shocks the von Neumann perfect gas theory is in good agreement with the data in our experiments, except for diffraction over single corners near transition where the famous persistence phenomenon is found. In this case the variation of specific heats does offer a partial explanation because by the reduction of γ with increased temperature regular reflexion is found to persist to larger values of ω_0 than for a perfect gas. We calculated the shift in ω_e due to this effect but it accounted for only about one third of the persistence for the $M_0 3$ and $M_0 4$ shocks – which were our strongest. This effect is not negligible and becomes of increasing importance with increasing shock strength but it is not an adequate explanation of the persistence in our data, nor it seems is viscosity, because elsewhere the von Neumann perfect gas theory agrees quite well with the data. Therefore it would appear that perfect gas theory still has something to add to the explanation.

This work is supported by the Australian Research Grants Committee.

REFERENCES

Bleakney, W. & Taub, A. H. 1949 *Rev. Mod. Phys.* **21**, 584.
Bryson, A. E. & Gross, R. W. F. 1961 *J. Fluid Mech.* **10**, 1.
Eggink, H. 1943 *Zentralstelle Wissenschaftliche Ber., Aachen*, no. 1850.
Griffith, W. C. & Bleakney, W. 1954 *Am. J. Phys.* **22**, 597.

GUDERLEY, K. G. 1947 *HQ Air Materiel Command, Wright Field, Dayton, Ohio, Tech. Rep.* F-TR-2168 ND.

GUDERLEY, K. G. 1962 *The Theory of Transonic Flow.* Pergamon Press.

GVOZDEAVA, L. G., BAZHENOVA, T. V., PREDVODITELEVA, O. A. & FOKEEV, V. P. 1969 *Astron. Acta* **14**, 503.

GVOZDEAVA, L. G., BAZHENOVA, T. V., PREDVODITELEVA, O. A. & FOKEEV, V. P. 1970 *Astron. Acta* **15**, 503.

HEILIG, W. H. 1969 *Shock Tube Symp., Phys. Fluids Suppl.* I, 1–154.

HENDERSON, L. F. 1964 *Aero. Quart.* **15**, 181.

HENDERSON, L. F. 1965 *Aero. Quart.* **16**, 42.

HENDERSON, L. F. 1966 *J. Fluid Mech.* **26**, 607.

HENDERSON, L. F. 1967 *Z. Flugwiss.* **15** (2), 57.

HENDERSON, L. F. & LOZZI, A. 1975 *J. Fluid Mech.* **68**, 139.

KAWAMURA, R. & SAITO, H. 1956 *J. Phys. Soc. Japan* **11**, 584.

LAW, C. K. & GLASS, I. I. 1971 *C.A.S.I. Trans.* **4**, 2.

LEAN, G. H. 1946 *Rep. Aero. Res. Comm.* no. 10629 G.B.

LOZZI, A. 1975 Transition between regular and Mach reflexion. Ph.D. thesis, University of Sydney.

MERRITT, D. L. 1968 *A.I.A.A. J.* **6**, 1208.

MESHKOV, E. E. 1970 *Fluid Dyn.* **5**, 554.

MÖLDER, S. 1971 *C.A.S.I. Trans.* **4**, 73.

NEUMANN, J. VON 1963 *Collected Works*, vol. 6. Pergamon.

PANTAZOPOL, D., BELLET, J. C. & SOUSTRE, J. 1972 *C.R. Acad. Sci., Paris*, **275**, A225.

POLACHEK, H. & SEEGER, R. J. 1951 *Phys. Rev.* **84**, 922.

SAKURAI, A. 1964 *J. Phys. Soc. Japan* **19**, 1440.

SEMENOV, A. H., SYSHCHIKOVA, M. P. & BEREZKINA, M. K. 1970 *Sov. Phys. Tech. Phys.* **15**, 795.

SMITH, L. G. 1945 Photographic investigations of the reflection of plane shocks in air. *O.S.R.D. Rep.* no. 6271.

SMITH, W. R. 1959 *Phys. Fluids* **2**, 533.

STERNBERG, J. 1959 *Phys. Fluids* **2**, 179.

WECKEN, F. 1949 *Z. angew. Math. Mech.* **29**, 147.

WEYNANTES, R. R. 1968 *Tech. Note Inst. Aerospace Studies, University of Toronto*, UTIAS 126.

WHITE, D. R. 1952 *Proc. 2nd Midwestern Conf. on Fluid Mech.*, p. 253. Columbus: Ohio State University Press.

WUEST, W. 1948 *Z. angew. Math. Mech.* **28**, 3.

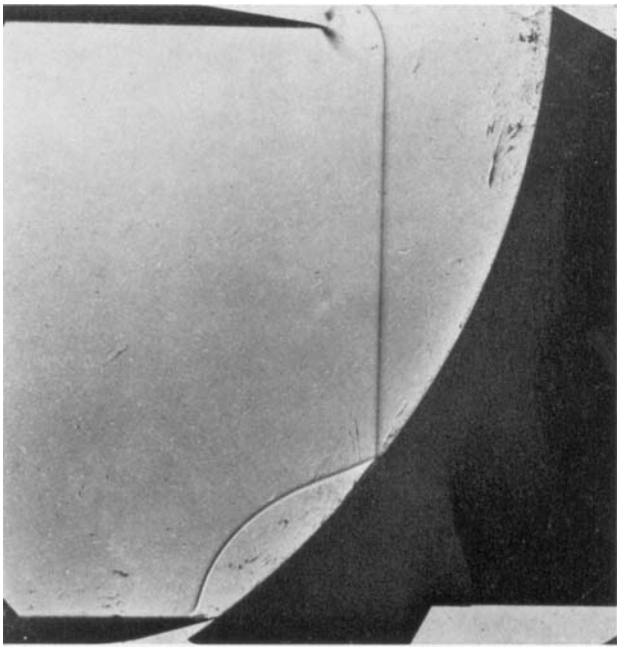

FIGURE 7. A double Mach reflexion DMR on a single concave corner (figure 2*b*) with surface radius $R = 7{\cdot}25$ cm, $M_0 = 4{\cdot}0 \pm 0{\cdot}03$, $\omega_0 = 36{\cdot}0 \pm 0{\cdot}2°$, $\omega_1' = 21{\cdot}5 \pm 1{\cdot}0°$, $\omega_1'' = 28{\cdot}0 \pm 1°$. Reynolds number based on diameter, $0{\cdot}5 \pm 0{\cdot}25 \times 10^6$, note that ω_0 is in the range $\omega_N < \omega_0 < \omega_e$.

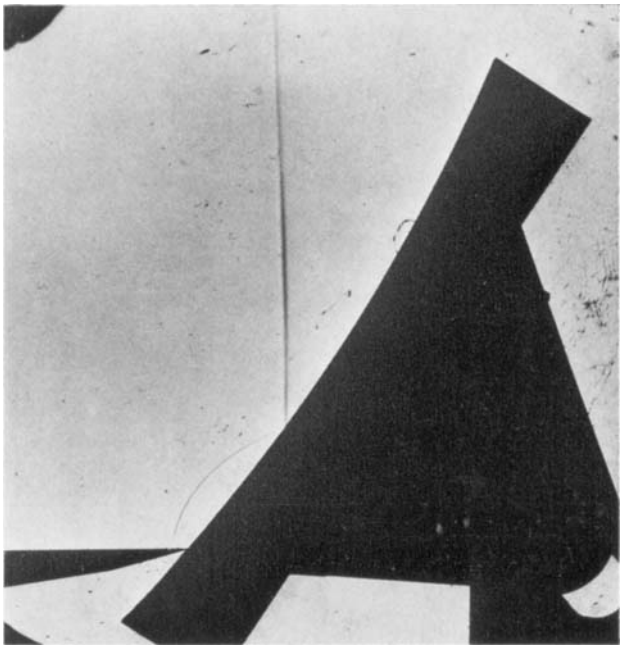

FIGURE 8. An apparent regular reflexion RR with a kink on a single concave corner (figure 2*b*) with surface radius $R = 19$ cm, $M_0 = 4{\cdot}0 \pm 0{\cdot}03$, $\omega_0 = 36{\cdot}8 \pm 0{\cdot}2°$, $\omega_1' = 28{\cdot}5 \pm 0{\cdot}5°$. Essentially the only difference between this flow and the one in figure 7 is the radius of the surface.

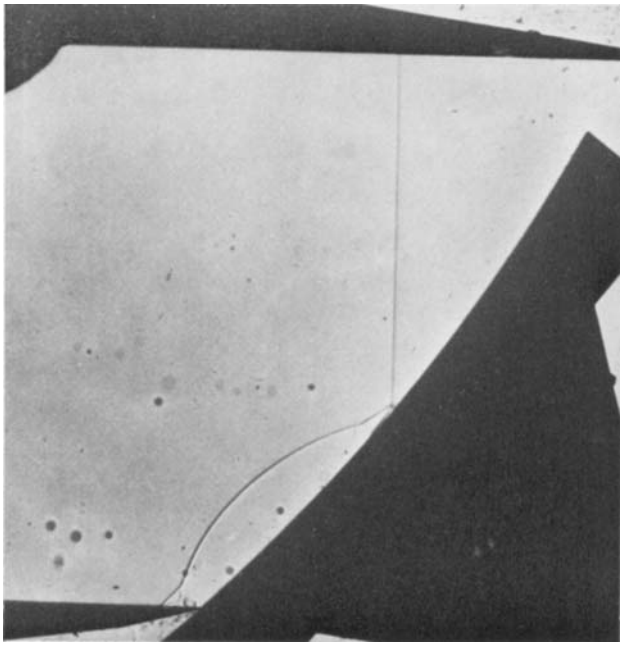

FIGURE 9. A double Mach reflexion DMR on a single concave corner (figure 2*b*) with surface radius $R = 19$ cm, $M_0 = 4{\cdot}0 \pm 0{\cdot}3$, $\omega_0 = 37{\cdot}5 \pm 0{\cdot}2°$, $\omega_1' = 20{\cdot}8 \pm 0{\cdot}5°$, $\omega_1'' = 32{\cdot}5 \pm 0{\cdot}5°$, Reynolds number based upon radius $1{\cdot}5 \pm 0{\cdot}5 \times 10^6$. Essentially the only difference between this flow and the one in figure 8 is an extra time delay to allow the DMR to become visible.

FIGURE 10. A regular-Mach reflexion RMR on a single concave corner (figure 2*b*) with surface radius $R = 7{\cdot}25$ cm, $M_0 = 1{\cdot}7 \pm 0{\cdot}1$, $\omega_0 = 41{\cdot}8 \pm 0{\cdot}2°$, $\omega_1' = 46 \pm 1°$, Reynolds number based upon radius $1{\cdot}6 \times 10^6$.

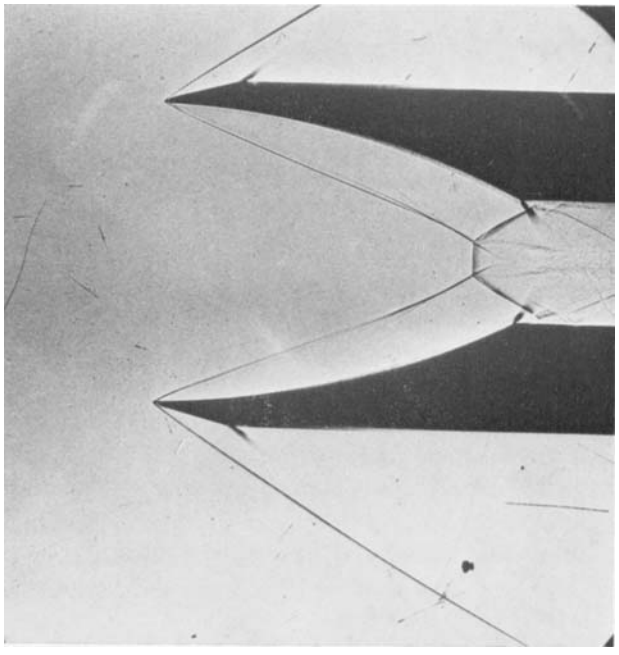

FIGURE 14. Symmetrical Mach reflexions at $M_0 = 2{\cdot}95 \pm 0{\cdot}05$ on model (f) (see figure 2) with concave surfaces of radius 10 cm and chordal distances across the surfaces 4·2 cm; $\omega_{01} = \omega_{02} = 30{\cdot}8 \pm 0{\cdot}5^\circ$; $\omega_1' = 39 \pm 1^\circ$; Reynolds number $2{\cdot}5 \pm 0{\cdot}5 \times 10^6$ cm^{-1}. Notice that the Mach stem is convex forward, and that the contact discontinuities at the confluences are initially deflected away from the centre-line.

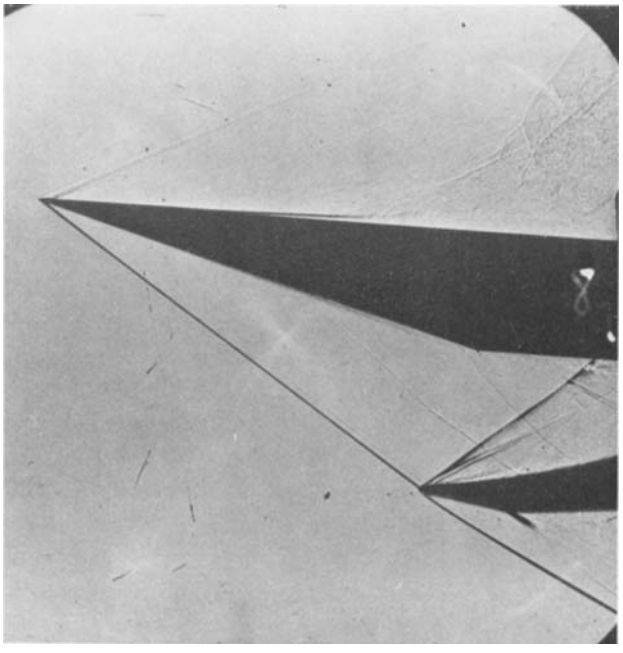

FIGURE 16. Complex Mach reflexion CMR with a weak kink in the reflected shock r; M_0 $2{\cdot}95 \pm 0{\cdot}05$; $\omega_0 = 38{\cdot}7 \pm 0{\cdot}2^\circ$; $\omega_1' = 33{\cdot}5 \pm 0{\cdot}5^\circ$; $\omega_1'' = 38{\cdot}0 \pm 0{\cdot}5^\circ$; Reynolds number $2{\cdot}5 \pm 0{\cdot}5 \times 10^6$ cm^{-1}. The Mach stem is too short to be resolved, and the contact discontinuity too close to the boundary layer; however CMR is implied by the measurements of ω_1' and ω_1''; notice that the difference is only $4\frac{1}{2}^\circ$ so the kink is very weak.